Catalysis Communications 149 (2021) 106176

Contents lists available at ScienceDirect

Catalysis Communications

journal homepage: www.elsevier.com/locate/catcom

Short communication

Dimethyl ether aromatization over nanosized zeolites: Effect of preparation method and zinc modification on catalyst performance

K.B. Golubev[a,*], K. Zhang[b], X. Su[b], N.V. Kolesnichenko[a], W. Wu[b]

[a] A.V. Topchiev Institute of Petrochemical Synthesis, RAS, Moscow 119991, Russia
[b] National Center for International Research on Catalytic technology, School of Chemistry and Material Sciences, Heilongjiang University, Harbin, Heilongjiang 150080, China

ARTICLE INFO

Keywords:
Dimethyl ether aromatization
Nanosized zeolite
Zinc modification
In situ seed-induced synthesis
Ultrasonic treatment
Acidity

ABSTRACT

Nanosized zeolites prepared by in situ seed-induced synthesis and samples prepared by ion exchanging commercial zeolites were successfully synthesized and modified with zinc. Their catalyst performance was investigated in the dimethyl ether aromatization at high pressures (up to 10 MPa) and various WHSV. The use of in situ seed-induced zeolite leads to a higher yield of arenes (39.1%) against 35.5% over the conventional sample. Zinc modification reduces the total yield of aromatics (by 22%), primarily BTX arenes (by 60%), compared to the parent zeolite. Such behavior correlates with a decrease in acidity and B/L ratio after modification.

1. Introduction

Aromatics are important feedstocks to manufacture basic organic chemicals and petrochemicals. Due to the continuous increase in demand, the world annual production of aromatics is keeping growing by about 3% and now exceeds 100 million t/y. Light arenes, such as benzene, toluene and xylenes, are the most prevalent in the chemical industry. Based on them, various technically valuable derivatives are obtained: synthetic materials (fibers, films) with enhanced thermal stability and mechanical strength, resins, rubbers, a wide range of surfactants and dyes, diverse stabilizers and plasticizers [1].

Currently, the modern industrial production of aromatics is mainly represented by the processes related to the processing of liquid oil fractions, which are catalytic reforming and pyrolysis, and to a lesser extent by coal carbonization processes [2,3]. In recent years, for the rational use of light hydrocarbons, as a part of associated petroleum gases, light alkanes aromatization processes have been actively developed [4,5]. One of the most successful technologies in this direction is the CYCLAR process. This is a joint project of UOP and British Petroleum to convert the propane-butane fraction into aromatics in the presence of pentasil zeolite-containing catalysts [6].

In order to provide a dynamically developing market with the required volume of aromatics, there is a tendency of constant growth of capacities for their production by engaging new sources of raw materials. At present, process developments aimed at the production of aromatic compounds on the basis of feedstocks being alternative to oil-derived hydrocarbons are particularly urgent for the world chemical industry. To date, there are technologies involving light aromatics production with a yield of 30–40% directly from the synthesis gas using bifunctional high-silica zeolites, such as ZSM-5 [7,8]. However, these technologies are complicated by the use of tubular reactors or two-sectional chemical reactors with a high proportion of gas flow circulation.

In addition, researches aimed at exploring the possibility of obtaining aromatic compounds by converting oxygen-containing organic substances, primarily alcohols and mixtures thereof, including bioethanol, are worth noting [9–13]. It is shown that the alcohols transformation is accompanied by the formation of liquid hydrocarbons containing 50–60 wt% arenes in the presence of zeolite catalysts modified with metal-oxide active components.

At the same time, since the idea of creating a single-step (direct) synthesis of dimethyl ether (DME) from CO and H_2 has been developed and successful outcome in this area has been achieved, interest in the implementation of new technologies for producing hydrocarbons based on DME, including technologies aimed at obtaining aromatics, has emerged [14,15]. To date, direct syngas to DME (STD) process is thermodynamically and economically more favorable than from methanol and is coming to the fore. The principal reactions involved in the STD process are methanol synthesis ($CO + 2H_2 \leftrightarrow CH_3OH$), methanol dehydration ($2CH_3OH \leftrightarrow CH_3OCH_3 + H_2O$) and water gas shift ($CO + H_2O \leftrightarrow CO_2 + H_2$). The combination of these reactions results in a synergistic effect for relieving the unfavorable thermodynamics for

* Corresponding author.
E-mail address: konstantin.golubev@ips.ac.ru (K.B. Golubev).

https://doi.org/10.1016/j.catcom.2020.106176
Received 19 August 2020; Received in revised form 25 September 2020; Accepted 28 September 2020
Available online 30 September 2020

methanol synthesis, because one of the products at each step is a reactant for another. This creates a strong driving force for the overall reaction ($3CO + 3H_2 \leftrightarrow CH_3OCH_3 + CO_2$), which allows a very high syngas conversion in one single pass. The STD, which simultaneously triggers methanol synthesis and in-situ dehydration, is integrated with hybrid bifunctional catalysts in a single reactor. This is an attractive alternative to the two-step process, which is imply the DME production through the intermediate methanol formation. In general, a higher one-pass syngas conversion and lower hydrogen demand (possibly at below H_2/CO ratio) in the feed stream with lower thermodynamic limitations and higher economical and theoretical significances make the STD attractive industrially. Also, the usages of a single reactor without purification and transportation units of methanol should reduce the capital costs for the DME production [16].

A modified ZSM-5 zeolite-based catalyst is used in the DME conversion to hydrocarbons, whereas the nature of the modifier and the method of its incorporation have a significant impact on the catalytic system performance. In addition, the nature of zeolite itself plays an important role in the performance of zeolite catalysts. The use of zeolites in the DME conversion to hydrocarbons is associated with their excellent catalytic behavior; nevertheless, in the presence of bulky molecules they are inefficient, since diffusion into zeolite microporous structures for such molecules becomes difficult. Only active sites close to the entrance of zeolite pores or on their external surface are accessible for bulky molecules. Recently, researchers have been interested in the use of nanocrystalline zeolites, which owing to the developed micropore surface area have a greater accessibility of active zeolite sites for reactants. The appearance of efficient nanozeolite catalysts became possible due to the use of advanced nanotechnology methods in the zeolite synthesis, which made it possible to obtain molecular sieves with shortened channels and micro/mesoporous lattice. It is through these methods that efficient nanosized catalytic systems with a hierarchical structure have been created over the last years. Nanosized ZSM-5 containing a significant amount of mesopores and strong acid sites has been successfully synthesized and studied in methanol and DME conversion [17,18]. The synergy and combined coordination of catalytic properties on the nanozeolite are related to its excellent catalyst performance for the production of high-octane gasoline (Research Octane Number = 137.2) enriched with components, such as toluene and xylene, while the benzene content is very low. Besides, the nanozeolite also exhibits a longer lifetime. Studies show that the nanosized catalyst is very promising for industrial applications. Hence, the seed-induced method has been explored and widely used for the preparation of nanozeolite by limiting the crystallite size of the final product [19]. This method produces the zeolite by template-free procedure providing short crystallization time and nonoccurrence of heterocrystals.

Apart from the seed-induced synthesis, an ultrasonic treatment is becoming a very promising way for obtaining nanosized catalysts. This strategy renders possible the large agglomerates to be reduced to particles with a size of less than 50 nm. Such catalytic systems based on ZSM-5 were successfully tested in the transformation of DME to light olefins by significantly increasing their activity [20].

In addition, adding the appropriate promoters to modify the zeolites is also recognized as an effective approach to improve their catalytic performance. Furthermore, the metal ions incorporation directly into the zeolite frame structure during its synthesis (in situ) contributes to the production of highly efficient catalysts with a high metal dispersion throughout the catalyst volume [21–23].

Zinc-containing zeolite catalytic systems are known to exhibit excellent performance in transformations of organic substances, in particular light alkanes and oxygenates, to aromatics. Zinc, due to its high dehydrogenation ability of the $ZnOH^+$ active component and along with that inexpensive price, is the most attractive metal promoter. The effect of a variety of zinc salts on the properties of HZSM-5 and the catalytic performances in MTA (methanol to aromatics) process are discussed in many papers. The results shows that the zeolites modified with zinc nitrate have a weaker acid sites and less strong acid sites, the BAS/LAS ratio declines, and the aromatics selectivity improves [10,21,24–27].

In the literature, there are next to nothing works concerning DTA (dimethyl ether to aromatics). In paper [15], we report the DTA process in the presence of microscale commercial ZSM-5-containing catalyst comprising 3 wt% zinc, with yielding no more 25% aromatics.

Summarizing the above, the main objectives of this study are to compare the preparation methods of nanosized zeolites in the DME aromatization and to determine the effect of zinc modification on a catalyst performance.

Therefore, this paper is devoted to the study of NZ-catalyst based on ZSM-5 and its in situ Zn-modified form as well as zinc-containing nanozeolite catalyst obtained by ultrasonic treatment in the DME transformation into aromatics concentrate. The effect of pressure, $WHSV_{DME}$ (hereinafter referred to as WHSV), zinc content and zinc modification technique are examined.

2. Experimental

2.1. Catalyst preparation

In this study, we used HNZ5 (H-form of the NZ (MFI-type zeolite)), Zn_2Al_8NZ5 and Zn_6Al_4NZ5 catalyst samples that were synthesized at the Key Laboratory of Chemical Engineering Process & Technology for High-Efficiency Conversion, School of Chemistry and Material Sciences, Heilongjiang University, Harbin, China, as well as H-ZSM-5 (MFI-type zeolite) manufactured by the Angarsk Plant of Catalysts and Organic Synthesis (Angarsk, Russia), and its modified form (Zn/ZSM-5).

Nanosized HNZ5, Zn_2Al_8NZ5 and Zn_6Al_4NZ5 MFI-type catalytic systems with Si/(Zn + Al) = 20 were synthesized using the latest method referred to as in situ seed-induced synthesis. According to this method, an aqueous solution was prepared from a mixture of tetraethyl orthosilicate (TEOS), aluminum isopropoxide (AIP) and tetrapropylammonium hydroxide (TPAOH) with a molar ratio of $1Al_2O_3$:$40SiO_2$:14.28TPAOH:$433H_2O$. The resulting solution was crystallized under microwave radiation at a temperature of 140 °C for 0.5 h. Afterwards, in the case of Zn_2Al_8NZ5 and Zn_6Al_4NZ5, the solution with precursors of zeolite grains (5 wt% with respect to the resulting gel) was added to the solution of SiO_2sol (Ludox, 30 wt% SiO_2 in water), $Zn(NO_3)_2 \cdot 6H_2O$, $NaAlO_2$, NaOH in the presence of deionized water under vigorous stirring. Zinc nitrate and sodium aluminate were added in such an amount that the original gel had the following molar composition: $200SiO_2$:2ZnO:$4Al_2O_3$:96NaOH:$10000H_2O$ in the case of Zn_2Al_8NZ5 and $200SiO_2$:6ZnO:$2Al_2O_3$:96NaOH:$10000H_2O$ in the case of Zn_6Al_4NZ5. Nanosized HNZ5 zeolite was prepared by the same method, but without the zinc nitrate addition. The final solution was crystallized in a Teflon-lined stainless steel autoclave at 180 °C for 24 h. The resulting zeolite was separated from the solution by centrifugation, washed with distilled water, dried at 110 °C and calcined at 550 °C for 3 h in a muffle furnace with air circulation in order to remove template residues. To obtain the H-form, the zeolite was subjected to ion exchange with 1 M ammonium nitrate solution followed by drying and calcination.

Zn/ZSM-5 catalyst was prepared by impregnating nanosized H-ZSM-5 (Si/(Zn + Al) = 20) MFI-type zeolite with zinc nitrate. In order to form nanoparticles, the parent zeolite was dispersed in distilled water under ultrasonic treatment in an Elmasonic P30 H ultrasonic bath (Germany) (ultrasound frequency, 80 kHz; power, 130 W) at a weight ratio of zeolite: water = 1:20. The treatment time was 1 h. After ultrasonic treatment, the zeolite was dried and calcined at 500 °C for 2 h. The zeolite was modified with zinc cations from an aqueous 0.1 M zinc nitrate solution by ion exchange.

Zinc weight percentages of the catalysts are shown in Table S2 (S = Supplementary material).

All the catalyst samples described above were pressed into tablets

and then calcined in air at 500 °C for 4 h. Afterwards, the tablets were crushed to obtain a fraction of 3–5 mm in size.

2.2. Catalyst characterization

X-ray powder diffraction (XRD) patterns of the catalyst samples were obtained on a Rigaku Rotaflex RU-200 X-ray unit (Japan) equipped with a rotating copper anode operated at a voltage of 50 kV and a current of 160 mA. Recording was performed using a Rigaku D/MAX-RC horizontal wide-angle goniometer according to the Bragg-Brentano scheme in the θ-2θ geometry. Scanning was performed at a 2θ angular range of 3°–50° at a speed of 4°/min in increments of 2θ = 0.04°. A graphite monochromator was used on the diffracted beam; the radiation wavelength was 1542 Å. A scintillation counter was used as a detector of diffracted X-ray radiation. Relative crystallinity was determined by the Standard test method for determination of relative crystallinity of ZSM-5 zeolite by XRD (ASTM International, D5758-01 (2015)) and calculated by Eq. (1):

$$\text{Crystallinity}\ (\%) = \frac{\sum S_{\text{modified,i}}}{\sum S_{\text{parent,i}}} \cdot 100 \quad (1)$$

where $S_{modified}$ and S_{parent} are integrated peak areas for the modified and parent zeolites in the range (2θ) of 22.5 to 25.0° from the XRD patterns; *i* is corresponding signal peak.

The morphological properties of the samples were characterized by scanning electron microscopy (SEM) using a JCM-6000 microscope operated at 30 kV. Prior to the analysis, the sample powders were fixed on the survey table using conductive scotch tape. The survey was performed in the secondary electron detection mode.

The elemental composition of the samples was studied using X-ray fluorescence (XRF) analysis on a Thermo ARL perform'x spectrometer (USA) equipped with a rhodium X-ray tube (operating modes were from 60 kV – 40 mA to 30 kV – 80 mA) and capable of determining the presence and concentration of elements with atomic numbers from F to U.

Low-temperature N_2 adsorption-desorption isotherms were tested on an Autosorb-1-MP apparatus (USA) at a temperature of −196 °C. Prior to the adsorption measurements, all of the samples were evacuated at a temperature of 350 °C and a pressure of $1.33 \cdot 10^{-3}$ Pa for 12 h. The specific surface area of the catalysts was determined according to BET at a relative partial pressure (p/p_0) of 0.02. The pore size distribution was calculated by BJH (Barrett-Joyner-Halenda) method using the desorption curve. The total pore volume was determined according to BJH at a relative partial pressure (p/p_0) of 0.99. The Horvath-Kawazoe method was used to establish the specific surface area and volume of micropores.

The acidic properties of the zeolites was studied by the temperature-programmed desorption of ammonia (NH_3-TPD) on an UNISIT USGA-101 instrument (Russia). A pre-calcined in air sample in an amount of 100 mg was loaded in a quartz reactor and heated in a flow of helium at 500 °C for 1 h. After cooling to 60 °C, the sample was saturated in the ammonia/nitrogen mixture stream for 15 min. Loosely bound ammonia was removed at 70 °C in the dry helium stream for 1 h; thereafter the sample was rapidly cooled to room temperature. Next, passing the helium stream (30 ml/min) through the sample, the NH_3-TPD profiles were recorded in the linear temperature rise mode up to 800 °C at a speed of 8 °C/min and detected using a thermal-conductivity detector.

The density of Brønsted (BAS) and Lewis (LAS) acid sites were determined by pyridine adsorbed FTIR (Py-FTIR) spectra measured on a Frontier FTIR spectrometer (PerkinElmer, USA). After pretreatment of the samples at 350 °C for 2 h under $1.33 \cdot 10^{-3}$ Pa, pyridine adsorption was performed at 90 °C. The spectra were recorded after desorption at 350 °C for 0.5 h. The amount of Brønsted (BAS) and Lewis (LAS) acid sites were estimated using integrating the area of the vibration bands at 1455 and 1545 cm^{-1}, respectively, and calculated by Eq. (2):

$$C = \frac{A}{\varepsilon} \cdot \frac{S}{m} \quad (2)$$

where C represents the density of acid sites ($mmol \cdot g^{-1}$), S is the surface area of the sample wafer (1.33 cm^2), A is the peak area of the vibration bands, m is the mass of a sample (g), and ε is the molar extinction coefficient (1.67 and 2.22 $cm \cdot \mu mol^{-1}$) for BAS and LAS, respectively.

The coke contents of spent zeolites were analyzed using a temperature-programmed oxidation (TPO) performed on a TGA/DSC3+ (Mettler Toledo, USA) instrument. The experimental procedure included outgassing 15 mg of sample at 200 °C for 1 h (a ramp rate of 10 °C/min) in 30 ml/min of He. Afterwards, the flow is switched to air at 30 ml/min. The TPO started at a ramp rate of 10 °C/min up to 650 °C for 90 min. The weight loss recorded between 350 and 650 °C was used to estimate the coke content.

2.3. Catalyst performance tests and characterization of the products

Catalytic tests of the samples were carried out on a high-pressure micropilot flow unit [28]. The catalyst weighing 3 g mixed with quartz in a volume ratio of 1: 2 was loaded into the isothermal zone of a reactor and heated in a nitrogen stream (5 l/h) at 400 °C for 4 h. The DME aromatization was carried out in the steel fixed-bed reactor in the synthesis gas stream at H_2/CO = 2 mol/mol as a medium at a temperature of 400–450 °C, a pressure of 3–10 MPa and WHSV = 2.7–26.7 h^{-1}. The DME concentration (C_{DME}) in the mixture of CO and H_2 at the reactor inlet was 45 vol%.

The rate of synthesis gas flow fed to the unit was regulated using a Bronkhorst F-232 M-RAD-33-V gas flow controller (the Netherlands). DME in the liquefied state was metered using a HPP 5001 high-pressure dosing pump (the Czech Republic). The temperature in the reactor was monitored by an OVEN TRM-210 automated temperature measuring/regulating controllers (Russia), and the pressure in the reactor was maintained by a mechanical Swagelok KPB1NOD412P200B0 back-pressure regulator (USA). The flow rate of the gaseous products was determined using a Shinagawa DC-1C-M gas meter (Japan).

The catalytic tests were completed within 5 h, the liquid products were discharged into receivers, and the mass and volume of the aqueous and organic phases were measured. Afterwards they were sent for analysis. Gases dissolved in liquid hydrocarbons were sampled using a special gas syringe and analyzed.

Chromatographic analysis of gas and liquid mixtures was performed using Crystalluxe 4000 M (Russia) apparatus as described in [29]. The high resolution chromatographic columns of the following types were used:

- inorganic gas products were analyzed on a packed column with the activated carbon phase of the SKT-4 (Meta-chrom, Russia) (column length, 1 m; i. d., 3 mm; particle size, 0.2–0.5 mm). The components were identified on TCD;
- organic gas products were analyzed on a Poraplot Q (Agilent, USA) open-tubular capillary column (styrene and divinylbenzene copolymer; column length, 25 m; i. d., 0.53 mm; film thickness, 20 μm). The components were identified on FID.
- liquid products (hydrocarbons) were analyzed on a Petrocol DH (Supelco, USA) open-tubular capillary column (bonded polydimethylsiloxane; column length, 100 m; i. d., 0.25 mm; film thickness, 0.5 μm). The components were identified on FID.

The hydrocarbons (C_6-C_{12} arenes, C_1-C_{12} paraffins, C_5-C_{12} naphthenes, C_2-C_{12} olefins), inorganic gases (H_2, CO, CO_2) and oxygenates (DME, methanol) were the main product groups identified according to their carbon number and nature.

Mass balance error of the catalytic tests is within 5%.

DME conversion (X) was calculated by Eq. (3):

$$X = \frac{n_0 - n}{n_0} \cdot 100, \ \% \quad (3)$$

where n_0 and n are the amount of DME moles at the inlet and outlet of the reactor, respectively.

Selectivity for products (S) was calculated through Eq. (4):

$$S = \frac{\mu_i \cdot N_i}{\sum \mu_i \cdot N_i} \cdot \ 100, \ \% \quad (4)$$

where μ_i is the molar fraction of product i, and N_i is the number of carbon atoms in a product molecule.

The yield of products (Y) was calculated by Eq. (5):

$$Y = \frac{X}{100} \cdot \frac{S}{100} \cdot \ 100, \quad \% \quad (5)$$

Hydrogen transfer index (HTI) was calculated by Eq. (6):

$$HTI = \frac{n_{alk.}}{n_{olef.}} \quad (6)$$

where $n_{alk.}$, $n_{olef.}$ Are the amount of moles of the formed C_{2+} alkanes and olefins, respectively.

3. Results and discussion

3.1. Structural and morphological properties

Fig. S1 presents the XRD patterns of the Zn-modified zeolite samples, and their relative crystallinity is given in Table S1. The XRD patterns show the characteristic diffraction peaks at 2θ = 7.92°, 8.80°, 14.78°, 23.10°, 23.90° and 24.40°, which indicate that the studied samples, regardless of the preparation method and the zinc content, are exclusively indexed to the structure of the MFI topology (JCPDS №42–0024). Moreover, no diffraction peaks for zinc oxide crystallites are observed from Zn_2Al_8NZ5 and Zn_6Al_4NZ5 samples. This fact indicates that Zn species can be highly dispersed on the surface of these catalysts. As can be seen from Table S1, the crystallinity of H-ZSM-5 nanosized catalyst and its modified form is slightly lower than that of HNZ5, Zn_2Al_8NZ5 and Zn_6Al_4NZ5 samples because of possible coverage of crystallites by Zn species after modification of the parent commercial zeolite with zinc. The zinc introduction into the zeolites framework affects the unit cell parameters and the unit cell volume (Vuc). Even more, the Vuc gradually decreased as the zinc content increased. This may be due to the shorter atomic radius of zinc (1.38 Å) than that of aluminum (1.43 Å). Based on the deviation of lattice cell parameters, it can be argued that the part of aluminum atoms in the zeolite framework are isomorphous substituted for zinc.

From the SEM data (Fig. S2), NZ5 zeolites are present in the form of agglomerates with irregular block morphology and consisting of cubic nanocrystals with a diameter of 50–100 nm. This fact confirms that they are nanosized materials. H-ZSM-5 and Zn/ZSM-5 have different size of agglomerates, which consists of aggregates and individual zeolite particles. The agglomerates of the H-ZSM-5 and Zn/ZSM-5 samples are morphologically inhomogeneous with the basis being large particles (about 2000 nm), but, along with them, nanosized particles (200–800 nm) are present in the group composition [30].

It should be noticed that the properties of Zn-containing zeolite catalysts are influenced by the Zn introduction method. When introducing zinc species by ion exchange, it is likely that the zinc cations have stabilized in the exchange positions of the zeolite with a high concentration of acid sites [10]. Compared to the conventional method using ion exchanging commercial zeolites, the in situ seed-induced synthesis provides a more dispersed distribution of the Zn species introduced into the zeolite [26]. Besides, the part of the Zn species were incorporated into the zeolite framework [27].

3.2. Textural properties and chemical composition

Fig. S3 provides the N_2 adsorption-desorption isotherms for the samples, and their textural properties and chemical composition are listed in Table S2.

As is seen from Fig. S3, the isotherms of the nanosized catalysts belong to the type I(a) according to the IUPAC classification, and they exhibit a steep increasing adsorption amount at the p/p_0 of 0.02. This corresponds to the transition of nitrogen molecules in the pore of the zeolites from monolayer to multilayer adsorption, which is characteristic of microporous zeolites. However, all the samples show a well-defined hysteresis loop in the range of p/p_0 = 0.45–1.0, which belong to the H4-type. It reveals the presence of a certain share of mesoporosity due to N_2 adsorption on the external surface of the crystallites and capillary condensation in spaces between the crystallites. The presence of hysteresis and its absence in the region of high relative pressures indicate that there is a limited connection of the porous system with the external surface of the zeolite crystallite.

As listed in Table S2, both the HNZ5 and Zn_2Al_8NZ5 are characterized by the largest surface. With increasing zinc content, the surface area decreases by 1.7 times. Zn_2Al_8NZ5 also has the largest volume of mesopores due to the accumulation of small nanocrystals [31].

From the textural properties of the synthesized zeolites listed in Table S2, it can be seen that the micropore volume and micropore surface area of the samples decreased after the incorporation of zinc species into the zeolites. This may be due to that parts of the highly dispersed zinc species being located on the external surface and/or the pore mouth of zeolite and thus reducing the accessibility of micropores because of their blockage. However, the mesopore volume of the samples increased, which may be attributed to the intergranular mesopores formed by the accumulation of ZnO nanoparticles after the chemical and thermal treatments [24]. The increased the specific surface area of the in situ seed-induced samples compared to conventional samples is caused by the higher dispersed nanosized crystallites themselves.

3.3. Acidity

The acidity of zeolite catalysts is one of the main parameters determining their behavior in the DME conversion into liquid hydrocarbons. Fig. S4 illustrates the NH_3-TPD profiles of the Zn-modified catalyst samples. As is seen, the profiles of all the samples exhibit two characteristic peaks in the low-temperature range of 222–246 °C and the high-temperature range of 394–447 °C, which can be attributed to the desorption of NH_3 on medium (I) and strong (II) acid sites, respectively. The acidic properties of nanosized catalysts strongly depend on the method of their preparation and the zinc content thereof. The amount of NH_3 desorbed and the distribution of acid sites over strength are given in Table S3. For nanozeolites as the zinc content is increased, the total acidity is reduced significantly. This indicates that a part of the intrinsic acid sites of ZSM-5 zeolites reacts with the incorporated Zn species, resulting in the dramatic reduction in the share of strong acid sites (I/II ratio in Table S3). In details, the Zn insertion into the zeolite leads to the interaction between Zn species and the surface hydroxyl groups (terminal Si(OH) and bridged Si(*OH*)Al) assigned to BAS, which become more pronounced with increasing Zn loading.

The pyridine FTIR spectra were obtained to determine the density of BAS and LAS of the catalysts. As seen in Fig. S5, the bands at 1545 cm^{-1} and 1454 cm^{-1} are associated with characteristic vibration peaks of pyridine molecule adsorbed at BAS and LAS. The amount of BAS and LAS as well as B/L ratio are shown in Table S3. The density of BAS and LAS were redistributed after the introduction of Zn into the zeolites, and larger amount of LAS were generated at expense of the BAS. Thus, the concentration of BAS sharply decreases, and the concentration of LAS (especially the medium ones) significantly increases with an increase of the Zn loading. Thus, B/L ratio reduces with increasing Zn

loading, suggesting that partial BAS are transferred to LAS. It is noted that the medium acid sites slightly decreases while the strong acid sites reduces much more considerably as the Zn loading increases. This suggests that the Zn introduction not only modified the concentration of LAS and BAS but also influenced the acidic strength distribution [32,33]. Such behavior can be explained by the formation $ZnOH^+$ Zn-containing species. The incorporated Zn species reacted with one proton of the BAS of the zeolite and thus formed the $ZnOH^+$ species through Zn—O—Al bonds. Other way, Zn-acid sites existed as Al—O—Zn^{2+}—O—Al via the interactions of one Zn^{2+} with two Al sites bridged by oxygen at nearby framework aluminum pairs [34,35]. In this way, the concentration of BAS and total acidity would significantly decrease compared with that of the parent zeolite.

It should also be noted that H-ZSM-5 and Zn/ZSM-5 nanosized catalysts have a much higher total acidity with a great proportion of medium acid sites.

3.4. Catalyst performance

The catalysts were investigated in the DME aromatization at various WHSV values. According to [15], DME is converted into an aromatics concentrate with a high yield at temperatures no lower than 400 °C. At higher temperatures, cracking reactions become more intense leading to enhanced gas formation and a drop in the total yield of the desired products. Therefore, the catalyst tests were run out at 400 °C. Selectivity for liquid hydrocarbons, aromatics content in the liquid hydrocarbons, DME conversion, and yields of aromatics are shown in Fig. 1 and Table 1.

These results demonstrate that variation in the reaction conditions leads to a considerable change in the main characteristics describing the behavior of the DME aromatization. The DME transformation into aromatics proceeds at a fairly high conversion over all the studied catalyst samples to form an aromatic compounds concentrate in the studied WHSV. Moreover, a change in pressure has a marked effect on the secondary reactions of the process and the redistribution of synthesis products. As exemplified by the Zn_2Al_8NZ5 catalytic system, an increase in pressure from 3 to 10 MPa has almost no effect on DME conversion. In the presence of Zn_2Al_8NZ5 and Zn_6Al_4NZ5 catalysts, the DME conversions above 99% are attained in the WHSV range of 2.7–26.7 h^{-1}. Owing to the molecular sieve properties of synthesized

Table 1
DME conversion, selectivity to gaseous hydrocarbons ($S_{gaseous\ HCs}$), BTX and C_{9+} aromatics yields, total yield of aromatics depending on the pressure and WHSV on the Zn-modified zeolite catalysts (C_{DME} = 45 vol%, H_2/CO = 2, T = 400°C).

P, MPa	WHSV, h^{-1}	X, %	$S_{gaseous\ HCs}$, %	Yield of aromatics, %		
				BTX	C_{9+}	Total
			Zn_2Al_8NZ5			
10	2.7	100	38.2	6.9	21.5	28.4
	5.3	100	42.9	8.7	20.4	29.1
	13.4	100	41.7	9.7	19.4	29.1
	26.7	100	41.8	10.2	16.5	26.7
3	2.7	100	29.2	12.4	20.6	33.0
	5.3	99.5	30.8	12.4	18.5	31.0
	13.4	100	35.3	12.9	17.0	29.9
	26.7	99.8	41.5	12.1	12.5	24.5
			Zn_6Al_4NZ5			
3	2.7	100	28.5	12.2	19.8	31.9
	5.3	99.4	28.8	9.4	20.3	29.7
	13.4	99.1	33.6	10.7	16.2	27.0
	26.7	99.4	39.3	12.5	11.3	24.1
			Zn/ZSM-5			
3	2.7	100	40.2	14.4	18.9	33.2
	5.3	100	38.0	13.2	18.2	31.5
	13.4	99.6	39.4	12.7	16.0	28.7
	26.7	94.8	49.8	12.1	11.9	24.0

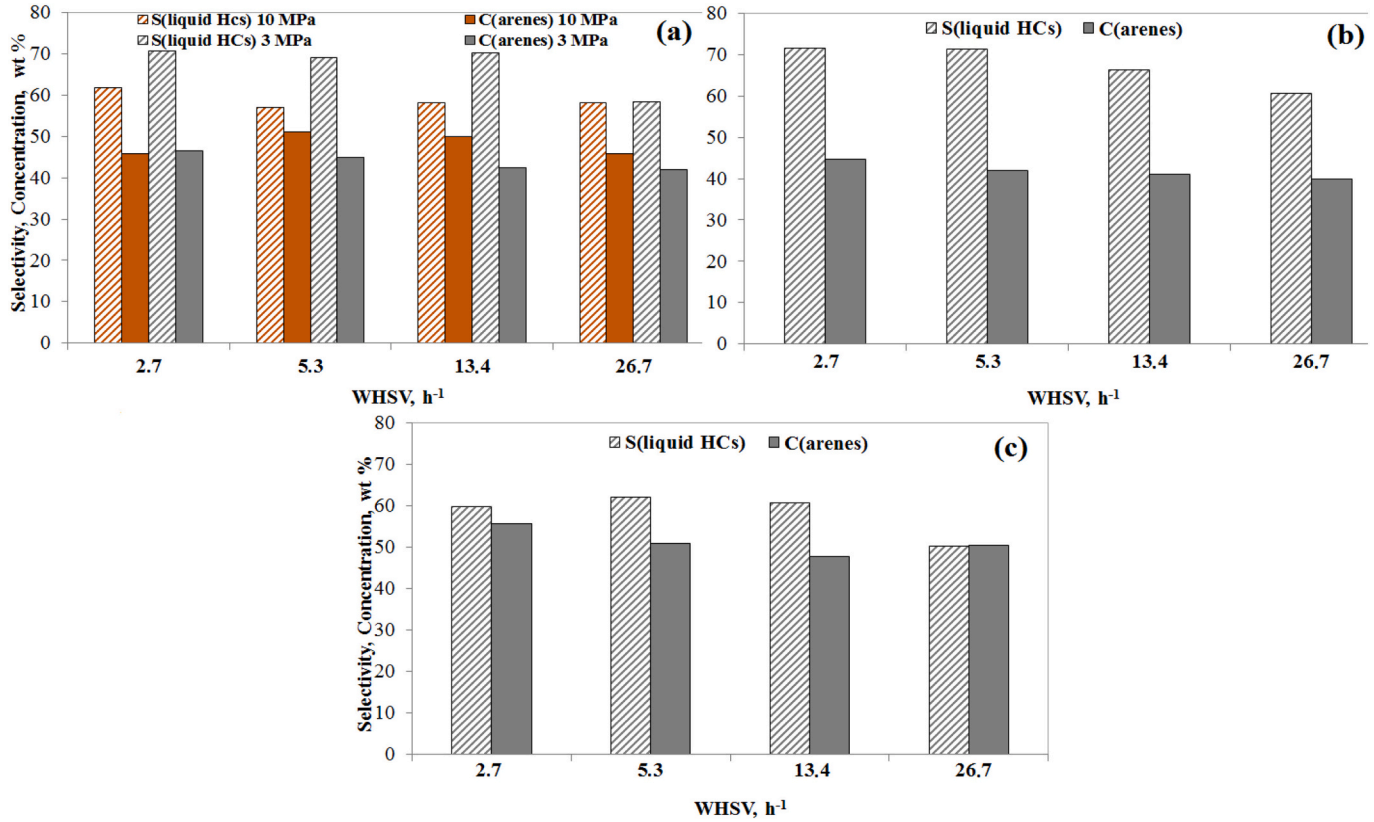

Fig. 1. WHSV effect on selectivity for liquid hydrocarbons (S(liquid HCs)) and aromatics content in the liquid hydrocarbons at T = 400°C: a) Zn_2Al_8NZ5 (P = 10 и 3 MPa); b) Zn_6Al_4NZ5 (P = 3 MPa); c) Zn/ZSM-5 (P = 3 MPa).

MFI-type zeolite catalysts, monocyclic alkylaromatic hydrocarbons with the number of carbon atoms from 6 to 12 are predominantly formed during the DME aromatization. Aromatics are largely represented by C_{9+} arenes and to a lesser extent by C_6–C_8 arenes. As is clear from Table 1, because of the reinforced alkylation reactions of the aromatic ring, a rise in pressure from 3 to 10 MPa leads to an increase in the yield of tri- and tetramethylbenzenes (C_{9+} arenes) from 12.5–20.6 to 16.5–21.5% with a simultaneous decrease in the yield of BTX (BTX = Benzene + Toluene + Ethylbenzene + Xylenes) aromatic compounds from 12.9–12.1 to 10.2–6.9%, respectively. In this case, an increase in pressure entails a reduction in the total yield of aromatics from 33.0–29.9 to 28.4–29.1% in the WHSV range of 2.7–13.4 h^{-1}. On the contrary, the occurrence of aromatization at WHSV = 26.7 h^{-1} is accompanied by an increase in the total yield of arenes from 24.5 to 26.7%, respectively. During testing of the Zn_2Al_8NZ5 sample the highest total yields of aromatics were obtained at 3 MPa. Importantly, the decrease in the pressure from 10 MPa to 3 MPa contributes to a marked decline in the selectivity to gaseous hydrocarbons. At WHSV = 2.7–13.4 h^{-1}, the pressure reduction leads to a fall in the selectivity to gaseous hydrocarbons by 23–28%. With a further increase in WHSV to 26.7 h^{-1}, the selectivity values are almost equal. For these reasons, the remaining catalytic systems synthesized by both in situ seed-induced method and by the conventional way (but using ultrasonic treatment) were accordingly tested at 3 MPa.

In order to determine the influence of Zn content on the selectivity to aromatic compounds, the catalyst performance of the Zn_2Al_8NZ5 and Zn_6Al_4NZ5 samples having the same Si/(Zn + Al) ratio but different Zn amounts (see Table S2) was compared. It was found that an increase in zinc concentration in the composition of NZ5 zeolites from 1.0 to 2.4 wt % leads to decrease in the total yield of aromatics by 3–10% depending on WHSV. However, at high WHSV values, the yields of aromatics for the Zn_2Al_8NZ5 and Zn_6Al_4NZ5 samples were almost equal. Interestingly, an increase in zinc concentration is accompanied by a slight fall in the selectivity to gaseous hydrocarbons amounting to 2–6% (Table 1).

As can be seen from Table 1, conventional zeolite catalyst processed by the ultrasonic treatment is characterized by a more evident drop in DME conversion at high WHSV values. At WHSV = 26.7 h^{-1} the DME conversion is 94.8% over the Zn/ZSM-5 sample. However, the total yield of aromatics over the Zn/ZSM-5 is close to that of NZ5 zeolites throughout the studied WHSV.

Compared with the nanosized zeolite systems prepared by the in situ seed-induced method, DME aromatization over the conventional nanosized catalyst prepared using ultrasonic treatment proceeds with a higher yield of BTX fraction, while the total yield of aromatics over the catalysts synthesized by different methods is roughly the same and differs by 5–10%. The yield of BTX arenes, including ethylbenzene, rises to 14.4 in the presence of the Zn/ZSM-5 catalyst, whereas for Zn_2Al_8NZ5 and Zn_6Al_4NZ5 it is around 11–12%. As is clear from Table 1, the catalytic systems synthesized by the in situ seed-induced method are more prone to the formation of C_{9+} arenes, the yield of which is above 20%. It is worth noting that the zeolite preparation method affects both the selectivity of aromatization process for liquid hydrocarbons and their composition (Fig. 1). The selectivity for liquid hydrocarbons over the Zn_2Al_8NZ5 and Zn_6Al_4NZ5 samples is far greater than that of the Zn/ZSM-5 sample. Indeed, in the presence of the NZ5 catalytic systems liquid hydrocarbon products are formed with a selectivity of 70.8–71.5% against 62.0% over the Zn/ZSM-5 catalyst (WHSV = 2.7 h^{-1}).

It should be noted that the NZ5 catalysts, compared with conventional system processed by ultrasonic treatment, are characterized by a reduced gas formation. As can be seen from Table 1, in the presence of the NZ5 samples, the selectivity to gaseous hydrocarbons is 29.2–41.5% (for Zn_2Al_8NZ5) and 28.5–39.3% (for Zn_6Al_4NZ5) throughout the studied WHSV, whereas that of Zn/ZSM-5 is 38.0–49.8%.

It is worth mentioning that the amount of syngas based on the mass balance at the outlet exceeds that at the inlet by 3–15%, depending on the process conditions. That is, during the reaction, the syngas accumulates. Moreover, a certain amount of carbon dioxide is formed. These are probably due to the proceeding water gas reaction (7) and the water gas shift reaction (8). Also, additional hydrogen can be formed by dehydrogenating naphthenes.

$$C + H_2O \leftrightarrow CO + H_2 \quad (7)$$

$$CO + H_2O \leftrightarrow CO_2 + H_2 \quad (8)$$

In this regard, it is safe to say that the syngas aromatization reaction does not occur under the studied conditions.

Table 2
DME conversion, selectivity to gaseous hydrocarbons, aromatics concentration in the liquid hydrocarbons, BTX and C_{9+} aromatics yields, total yield of aromatics on the parent zeolite catalysts (C_{DME} = 45 vol%, H_2/CO = 2, T = 400°C, P = 3 MPa, WHSV = 2.7 h^{-1}).

X, %	$S_{gaseous\ HCs}$, %	C_{arenes}, wt%	Yield of aromatics, %		
			BTX	C_{9+}	Total
		HNZ5			
100	44.1	70.0	19.8	19.3	39.1
		H-ZSM-5			
100	47.3	67.3	18.7	16.8	35.5

In order to determine the effect of the zinc incorporation on the aromatization performance, experimental tests in the presence of H-form parent zeolites (HNZ5 and H-ZSM-5) were carried out. The results are given in Table 2.

As can be seen from Table 2, the parent zeolites unmodified with zinc exhibit high performance in the DME aromatization. At WHSV = 2.7 h^{-1}, the DME conversion is 100% over all the tested samples. The total yield of aromatic compounds is 35.5 on H-ZSM-5, which is approximately 7% higher than that of corresponding Zn-modified form. The highest total yield is observed on the HNZ5 zeolite (39.1%), which is 18–22% higher than that of the Zn_2Al_8NZ5 and Zn_6Al_4NZ5 catalysts. It is important to note that the zinc absence in the catalysts facilitates a more selective BTX arenes production, whose share in the reaction products exceeds that of C_{9+} arenes. The HNZ5 sample is the most selective to the BTX arenes.

However, one of the disadvantages of unmodified systems is the increased selectivity to gaseous hydrocarbons negatively affecting the overall process selectivity. This trend is most pronounced on the NZ5 catalysts, where the zinc absence results in an enhanced gas formation by 50–55% (44.1% against 29.2 and 28.5%). In the case of conventional system, the zinc introduction into the parent zeolite structure has a weaker effect on the gas formation. Thus, on the H-ZSM-5 and Zn/ZSM-5, the selectivity for gaseous hydrocarbons is 47.3 and 40.2%, respectively. This phenomenon is attributable to a decrease in the total acidity of the samples, primarily due to a decrease in the number of strong acid sites after Zn modification. These sites promote C—C bond cleavage in liquid-phase aromatization products.

Fig. 2 illustrates the distribution of hydrocarbons in the DME aromatization products.

As shown in Fig. 2, the method of preparing nanosized catalytic systems affects the group composition of the resulting hydrocarbons. The catalysts samples synthesized by the in situ seed-induced method are characterized by a higher concentration of olefins and naphthenes (except for HNZ5) in the reaction products and a reduced content of alkanes, including methane, compared with the samples synthesized by the conventional method. For example, the total content of olefins over the Zn_2Al_8NZ5 and Zn_6Al_4NZ5 samples is 4.0, 5.3 and 5.1% and the content of naphthenes is 0.8, 3.7 and 3.4%, respectively, whereas the total olefins content over the H-ZSM-5 and Zn/ZSM-5 systems is 1.6 and 2.8% and the content of naphthenes is 1.0 and 2.3%, respectively. The amount of C_{2+} alkanes over the HNZ5, Zn_2Al_8NZ5 and Zn_6Al_4NZ5

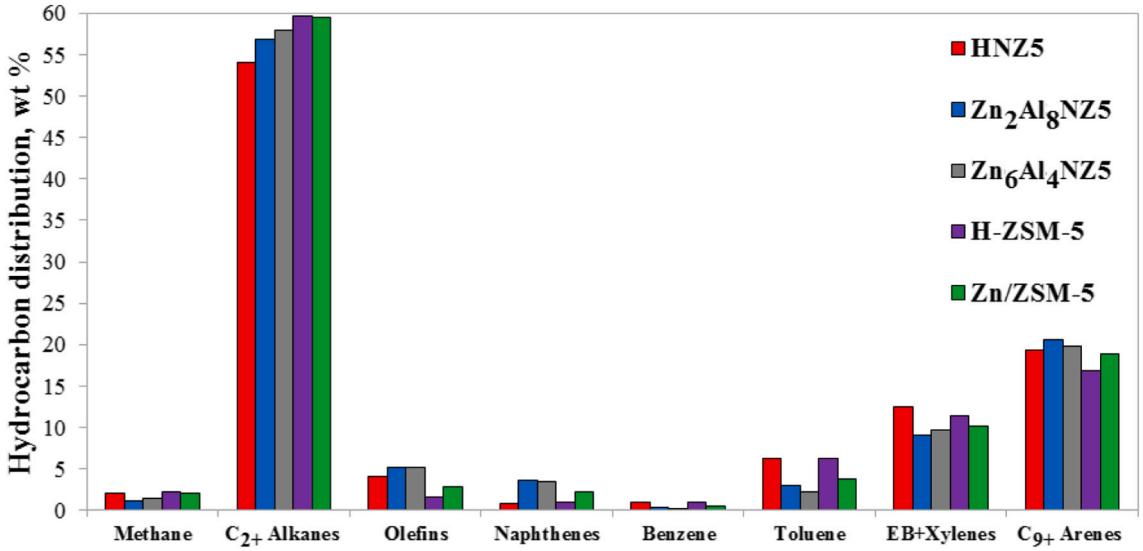

Fig. 2. Hydrocarbon distribution of the DME aromatization products (T = 400°C, P = 3 MPa, WHSV = 2.7 h^{-1}).

catalysts is 54.0, 56.9 and 58.0 with methane content being equal to 2.0, 1.2 and 1.5% respectively. Over the H-ZSM-5 and Zn/ZSM-5 samples, the total content of C_{2+} alkanes in the reaction products is 59.6 and 59.5%, respectively; the content of methane is 2.2 and 2.0%, respectively. The content of individual aromatic compounds fully correlates with the results described above and presented in Table 1 and Table 2.

The increased content of C_{2+} alkanes in the reaction products is most likely due to the fact that olefins are much more easily hydrogenated than cyclized to aromatics in the syngas medium. The higher selectivity for C_{2+} alkanes on the Zn-modified samples compared to that on the unmodified zeolites can be explained by the excellent H_2 heterolysis ability of the $ZnOH^+$ species. H_2 is adsorbed and dissociated on the $ZnOH^+$ species followed by hydrogenation of olefin intermediates [18]. Therefore, in the presence of $ZnOH^+$ species, the H_2 activation and hydrogenation reactions are promoted, immediately increasing the selectivity to paraffins while reducing the selectivity for aromatics. Hence, the paraffin formation and aromatization are competitive reactions.

Importantly, at TOS (time on stream) = 5 h (WHSV = 2.7 h^{-1}), there is no noticeable decrease in the activity of the catalyst. This is evident from the DME conversion values, which are 99–100%. The drop in conversion and yield with increasing WHSV is due to a decrease in residence time rather than the formation of coke deposits. In addition, it is important to note that the use of nanosized catalytic systems facilitates increased resistance to coke formation, since the larger mesopore volume of nanosized zeolites effectively promote the diffusion rate and thus inhibit the carbon production. We carried out lifetime testing the HNZ5 and Zn_2Al_8NZ5 at WHSV = 2.7 h^{-1} for 48 h, whereafter these samples were analyzed by TPO for coke content. As can be seen from Fig. S6, decline in the DME conversion and aromatics selectivity on the HNZ5 are more greater than those on the Zn_2Al_8NZ5 with TOS of 48 h. On the HNZ5, the DME conversion steadily reduces from 100 to 96.7%, all while the selectivity to aromatics drops from 39.1 to 35.5% (by 10%). The product selectivity is more stable on the Zn_2Al_8NZ5 and reduces by merely 3% after 48 h (from 33.0 to 32.0%), with the DME conversion over time no falling below 98.5%. This may be attributed to the high hydrogenation activity of well-dispersed $ZnOH^+$ species exhibiting the lower aromatization ability. Therefore, the formation of carbon precursor aromatics is suppressed, which further inhibits the formation of graphite carbon [18].

Fig. S7 demonstrates the TPO profiles of the zeolites after 48 h aromatization performance. Fig. S7(a) depicts the weight loss during the TPO, wherein the coke combustion was assumed to start at 350 °C. Fig. S7(b) reflects the corresponding heat effects. The weight loss lower 350 °C was caused by both removing the adsorbed water and loosely bound hydrocarbons and burning the hydrocarbons. Appearing a marked *exo*-effect (Fig. S7(b) (the peaks at 445–510 °C on the HNZ5 and 410–510 °C on the Zn_2Al_8NZ5) is resulted from the oxidation of the high-temperature coke deposits to the formation of gas products. The TPO profiles indicate that the nature of coke is very similar for the studied catalysts. As is clear from the weight loss curves, the coke content on the Zn_2Al_8NZ5 is approximately 30% lower than that of HNZ5. The weight loss in the range of 350–650 °C on the Zn_2Al_8NZ5 is 8.0%, whereas on the HNZ5 is 10.5%. This points to the fact that the zinc modification slows down the deactivation of the zeolite catalyst.

Fig. 3 displays the values of HTI (hydrogen transfer index) calculated by Eq. 4 for the catalysts used in the DME aromatization.

It is seen that all the catalyst samples used are characterized by high HTI values, indicating that H-transfer reactions prevail over dehydrogenation reactions in the DME aromatization. However, in the presence of the NZ5 catalytic systems H-transfer reactions are less pronounced than those on the conventional samples. Meanwhile, zinc introduction into the zeolite results in a decrease in HTI. It is most likely attributed to the fact that zinc species form new strong LAS by interacting with the zeolite BAS responsible for H-transfer reactions. The HTI values of the HNZ5, Zn_2Al_8NZ5 and Zn_6Al_4NZ5 samples are 13.4,

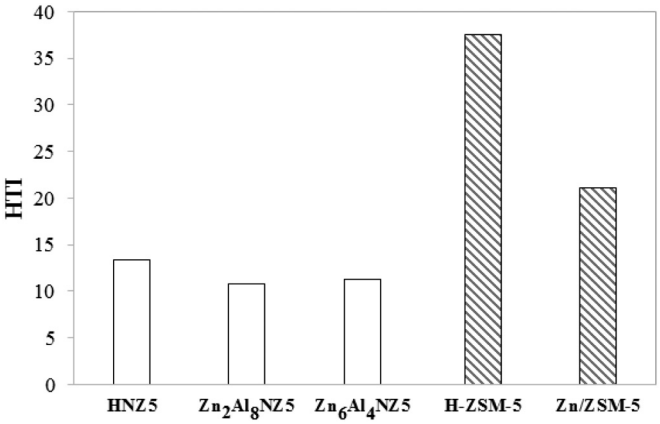

Fig. 3. HTI values of the catalysts used in the DME aromatization (T = 400°C, P = 3 MPa, WHSV = 2.7 h^{-1}).

10.8 and 11.3, respectively. The highest HTI value is observed for the H-ZSM-5 (37.5) against 21.1 on the Zn/ZSM-5. Based on these data, it can be stated that H-transfer reactions are primarily responsible for formation of aromatic compounds under the process conditions.

4. Conclusion

This work provides an efficient green chemical process for the synthesis of nanosized ZSM-5 zeolites, which are widely used in the petrochemical industry. In this work, nanosized ZSM-5 zeolites and Zn-modified forms thereof were successfully synthesized via various methods and their morphological, textural and acidic properties were studied by XRD, SEM, N_2 adsorption-desorption, NH_3-TPD and Py-FTIR techniques. Catalytic activities in the DME aromatization over the in situ seed-induced samples and the conventional samples prepared by ion exchange procedure using ultrasonic treatment were compared. The in situ seed-induced zeolite facilitates a higher aromatics yield (39.1%) as opposed to that on the conventional sample (35.5%). The preparation method influences the hydrocarbon distribution. Except for arenes, the in situ seed-induced zeolites give an increased amount of olefins, whereas the conventional ion-exchanged samples produce a greater amount of paraffins. Zinc modification of the zeolites reduces the total yield of aromatics (by 22%), primarily BTX arenes (by 60%). Aromatics yield can be controlled by acidity and B/L ratio that affected by zinc introduction. The lifetime testing and TPO analysis has revealed that the zinc modification slows down the deactivation of the catalyst by suppressing coke formation. It was shown that it is possible to synthesize aromatic hydrocarbons from DME with a fairly high total yield at pressures up to 10 MPa. Our studies demonstrated that the nature of the parent zeolite and the method of preparing catalytic system have a significant impact on DME aromatization. This makes it possible to control the yield and distribution of the targeted synthesis products.

Declaration of Competing Interest

The authors declare that they have no competing interests.

Acknowledgements

This work was supported by the Russian Science Foundation (project no. 17-73-30046). This work was performed using the equipment of the Shared Research Center «Analytical center of deep oil processing and petrochemistry of TIPS RAS.

Appendix A. Supplementary data

Supplementary data to this article can be found online at https://doi.org/10.1016/j.catcom.2020.106176.

References

[1] N. Martin, Y. Tobe, Novel aromatics: from synthesis to applicatons, ChemPlusChem. 82 (2017) 943–944, https://doi.org/10.1002/cplu.201700262.
[2] H.R. Omran, S.M. El-Marsafy, F.H. Ashour, E.F. Abadir, Economic evaluation of aromatics production, a case study for financial model application in petrochemical projects, Egypt. J. Petr. 26 (2017) 855–863, https://doi.org/10.1016/j.ejpe.2015.03.013.
[3] H. Peng, X.-J. Zhang, X.-F. Mao, Research on the production of aromatic hydrocarbon via hydroreforming a light fraction in direct coal liquefaction oil, Energy and Fuels 29 (2015) 86–90, https://doi.org/10.1021/ef502146a.
[4] A.A. Vosmerikov, L.N. Vosmerikova, I.G. Danilova, A.V. Vosmerikov, Production of aromatic hydrocarbons from C_3, C_4-alkanes over zeolite catalysts, J. Siber. Fed. Univer.: Chemistry 12 (2019) 144–154, https://doi.org/10.17516/1998-2836-0114.
[5] E.I. Khasanova, I.F. Nazmieva, A.S. Ziyatdinov, I.I. Salakhov, A.Y. Kopylov, A study of propane aromatization on a zeolite-containing catalyst with different Si/Al ratios, Petr. Chem. 52 (2012) 79–85, https://doi.org/10.1134/S0965544112020107.
[6] G. Gianetto, R. Monque, R. Galiasso, Transformation of LPG into aromatic hydrocarbons and hydrogen zeolite catalysts, Cat. Rev.: Sci. Engineer. 36 (1994) 271–304, https://doi.org/10.1080/01614949408013926.
[7] K. Cheng, W. Zhou, J. Kang, S. He, S. Shi, Q. Zhang, Y. Pan, W. Wen, Y. Wang, Bifunctional catalysts for one-step conversion of syngas into aromatics with excellent selectivity and stability, Chem 3 (2017) 334–347, https://doi.org/10.1016/j.chempr.2017.05.007.
[8] B. Zhao, P. Zhai, P. Wang, J. Li, T. Li, M. Peng, M. Zhao, G. Hu, Y. Yang, Y.-W. Li, Q. Zhang, W. Fan, D. Ma, Direct transformation of syngas to aromatics over Na-Zn-Fe_5C_2 and hierarchical HZSM-5 tandem catalysts, Chem 3 (2017) 323–333, https://doi.org/10.1016/j.chempr.2017.06.017.
[9] T. Wang, X. Tang, X. Huang, W. Qian, Y. Cui, X. Hui, W. Yang, F. Wei, Conversion of methanol to aromatics in fluidized bed reactor, Cat. Today 233 (2014) 8–13, https://doi.org/10.1016/j.cattod.2014.02.007.
[10] I. Pinilla-Herrero, E. Borfecchia, J. Holzinger, U.V. Mentzel, F. Joensen, K.A. Lomachenko, S. Bordiga, C. Lamberti, G. Berlier, U. Olsbye, S. Svelle, J. Skibsted, P. Beato, High Zn/Al ratios enhance dehydrogenation vs hydrogen transfer reactions of Zn-ZSM-5 catalytic systems in methanol conversion to aromatics, J. Cat. 362 (2018) 146–163, https://doi.org/10.1016/j.jcat.2018.03.032.
[11] L. Yu, S. Huang, S. Zhang, Z. Liu, W. Xin, S. Xie, L. Xu, Transformation of isobutyl alcohol to aromatics over zeolite-based catalysts, ACS Cat. 2 (2012) 1203–1210, https://doi.org/10.1021/cs300048u.
[12] V.F. Tret'yakov, R.M. Talyshinskii, A.M. Ilolov, A.D. Budnyak, Production of aviation fuel by bioethanol conversion on zeolite catalysts, Petr. Chem. 56 (2016) 224–229, https://doi.org/10.1134/S0965544116030130.
[13] T.Q. Hoang, X. Zhu, T. Danuthai, L.L. Lobban, D.E. Resasco, R.G. Mallinson, Conversion of glycerol to alkyl-aromatics over zeolites, Energy and Fuels 24 (2010) 3804–3809, https://doi.org/10.1021/ef100160y.
[14] N.V. Kolesnichenko, Z.M. Bukina, N.A. Markova, O.V. Yashina, G.I. Lin, A.Ya. Rozovskii, L.E. Kitaev, V.V. Yushchenko, Synthesis of gasoline from syngas via dimethyl ether, Kinet. Cat. 48 (2007) 789–793, https://doi.org/10.1134/S0023158407060043.
[15] K.B. Golubev, S.P. Bedenko, A.D. Budnyak, A.M. Ilolov, V.F. Tret'yakov, R.M. Talyshinskii, A.L. Maksimov, S.N. Khadzhiev, Conversion of oxygenates to aromatic hydrocarbons on a commercial zeolite catalyst: comparison of ethanol and dimethyl ether, Rus, J. Appl. Chem. 92 (7) (2019) 918–923, https://doi.org/10.1134/S1070427219070061.
[16] K. Saravanan, H. Ham, N. Tsubaki, J.W. Bae, Recent progress for direct synthesis of dimethyl ether from syngas on the heterogeneous bifunctional hybrid catalysts, Appl. Cat. B: Env. 217 (2017) 494–522, https://doi.org/10.1016/j.apcatb.2017.05.085.
[17] K. Zhang, X. Su, W. Wu, S.A. Kurumov, Y.M. Snatenkova, Z.M. Bukina, N.V. Kolesnichenko, S.N. Khadzhiev, Zinc-modified ZSM-5 nanozeolites synthesized by the seed-induced method: interrelation of their textural, acidic, and catalytic properties in DME conversion to hydrocarbons, Petr. Chem. 57 (2017) 1036–1042, https://doi.org/10.1134/S0965544117120179.
[18] X. Su, K. Zhang, Yu. Snatenkova, Z. Matieva, X. Bai, N. Kolesnichenko, W. Wu, High-efficiency nano [Zn,AlZSM-5] bifunctional catalysts for dimethyl ether conversion to isoparaffin-rich gasoline, Fuel Proc. Tech. 198 (2020) 106242, , https://doi.org/10.1016/j.fuproc.2019.106242.
[19] M.H. Nada, S.C. Larsen, Insight into seed-induced-assisted template free synthesis of ZSM-5 zeolites, Micropor. Mesopor. Mater. 239 (2017) 444–452, https://doi.org/10.1016/j.micromeso.2016.10.040.
[20] T.I. Batova, T.K. Obukhova, N.V. Kolesnichenko, S.A. Nikolaev, Effect of ultrasonic treatment on the physicochemical and catalytic properties of rhodium-chitisan/HTSVM catalysts in dimethyl ether conversion to lower olefins, 59 (9) (2019) 1017–1022, https://doi.org/10.1134/S0965544119090032.
[21] G. Wang, W. Wei, W. Zan, X. Bai, W. Wang, X. Qi, O.V. Kikhtyanin, Preparation of Zn-modified nano-ZSM-5 zeolite and its catalytic performance in aromatization of 1-hexene, Trans. Nonferrous Met. Soc. China 25 (2015) 1580–1586, https://doi.org/10.1016/S1003-6326(15)63761-X.
[22] Y. Fang, X. Su, X. Bai, W. Wei, G. Wang, L. Xiao, A. Yu, Aromatization over nanosized Ga-containing ZSM-5 zeolites prepared by different methods: effect of acidity of active Ga species on the catalytic performance, J. Energy Chem. 26 (2017) 768–775, https://doi.org/10.1016/j.jechem.2017.03.014.
[23] X. Su, W. Zan, X. Bai, G. Wang, W. Wu, Synthesis of microscale and nanoscale ZSM-5 zeolites: effect of particle size and acidity of Zn modified ZSM-5 zeolites on aromatization performance, Cat. Sci. Tech. 7 (2017) 1943–1952, https://doi.org/10.1039/c7cy00435d.
[24] K. Wang, M. Dong, X. Niu, J. Li, Z. Qin, W. Fan, J. Wang, Highly active and stable Zn/ZSM-5 zeolite catalyst for the conversion of methanol to aromatics: effect of support morphology, Cat. Sci. Tech. 8 (2018) 5646–5656, https://doi.org/10.1039/c8cy01734d.
[25] G.Q. Zhang, T. Bai, T.F. Chen, W.T. Fan, X. Zhang, Conversion of methanol to light aromatics on Zn-modified nano-HZSM-5 zeolite catalysts, Ind. Eng. Chem. Res. 53 (2014) 14932–14940, https://doi.org/10.1021/ie5021156.
[26] Y. Ni, A. Sun, X. Wu, G. Hai, J. Hu, T. Li, G. Li, The preparation of nanosized H[Zn,Al]ZSM-5 zeolite and its application in the aromatization of methanol, Microp. Mesop. Mater. 143 (2011) 435–442, https://doi.org/10.1016/j.micromeso.2011.03.029.
[27] X. Niu, J. Gao, Q. Miao, M. Dong, G. Wang, W. Fan, Zh. Qin, J. Wang, Influence of preparation method on the performance of Zn-containing HZSM-5 catalysts in methanol-to-aromatics, Microp. Mesop. Mater. 197 (2014) 252–261, https://doi.org/10.1016/j.micromeso.2014.06.027.
[28] L.E. Kitaev, V.V. Yushchenko, Z.M. Bukina, D.A. Ionin, N.V. Kolesnichenko, S.N. Khadzhiev, Physicochemical and catalytic characteristics of La-H-ZSM-5 zeolite in converting dimethyl ether to the mixtures of gasoline hydrocarbons: effect of ion exchange conditions, Rus. J. Phys. Chem. A 88 (2014) 381–385 10.1134S003602441403011X.

[29] K.B. Golubev, M.V. Magomedova, Gasoline manufacture from products of partial oxidation of methane on MFI-type zeolite catalysts, Petr. Chem. 57 (2017) 562–568, https://doi.org/10.1134/S0965544117100073.
[30] N.V. Kolesnichenko, O.V. Yashina, N.N. Ezhova, G.N. Bondarenko, S.N. Khadzhiev, Nanodispersed suspensions of zeolite catalysts for converting dimethyl ether into olefins, Russian J. Phys. Chem. A. 92 (2018) 118–123, https://doi.org/10.1134/S0036024418010120.
[31] K.A. Sashkina, Q. Zhiye, W. Wu, A.B. Ayupov, A.I. Lysikov, E.V. Parkhomchuk, The effect of H_2O/SiO_2 ratio in precursor solution on the crystal size and morphology of zeolite ZSM-5, Microp. Mesop. Mater. 244 (2017) 93–100, https://doi.org/10.1016/j.micromeso.2017.02.060.
[32] M. Fattahi, R.M. Behbahani, T. Hamoule, Synthesis promotion and product distribution for HZSM-5 and modified Zn/HZSM-5 catalysts for MTG process, Fuel 181 (2016) 248–258, https://doi.org/10.1016/j.fuel.2016.04.120.
[33] R. Ramos, A. Garcia, J.A. Botas, D.P. Serrano, Enhanced production of aromatic hydrocarbons by rapeseed oil conversion over Ga and Zn modified ZSM-5 catalysts, Ind. Eng. Chem. Res. 55 (2016) 12723–12732, https://doi.org/10.1021/acs.iecr.6b03050.
[34] S. Almutairi, B. Mezari, P. Magusin, E. Pidko, Structure and reactivity of Zn-modified ZSM-5 zeolites: the importance of clustered cationic Zn complexes, ACS Catal. (1) (2012) 71–83, https://doi.org/10.1021/cs200441e.
[35] J. Xiu, N. He, W. Zhou, L. Lin, G. Liu, C. Liu, J. Wang, Q. Xin, G. Xiong, H. Guo, Isobutane aromatization over a complete Lewis acid Zn/HZSM-5 zeolite catalyst: performance and mechanism, Catal. Sci. Tech. 8 (2018) 4018–4029, https://doi.org/10.1039/C8CY00917A.